

The role of the continuum and the spurious 1^- transitions in incoherent $\mu^- - e^-$ conversion rate calculations^{*)}

P. PAKONSTANTINO, J. WAMBACH

*Institut für Kernphysik, Technische Universität Darmstadt,
D-64289 Darmstadt, Germany*

O. CIVITARESE

*Departamento de Física, Universidad Nacional de La Plata,
c.c. 67 1900 La Plata, Argentina*

T.S. KOSMAS

Department of Physics, University of Ioannina, GR-45110 Ioannina, Greece

Received 18 April 2006

By using the Continuum RPA (CRPA) method, the incoherent transition strength of the exotic $\mu^- - e^-$ conversion in nuclei is investigated. The question whether excited nuclear states lying high in the continuum give an important contribution to the incoherent rate is addressed. Results for ^{40}Ca are compared with those obtained previously for ^{208}Pb . For both nuclei we then investigate in detail the admixture of spurious components in the rate coming from 1^- excitations, within the self-consistent CRPA with Skyrme interactions as well as within a less consistent version. We employ and compare two methods for removing the spurious strength: the use of effective operators, as done in a previous work for ^{208}Pb , or simply the exclusion of the spurious state appearing close to zero energy. In all cases, the correction achieved is quite large.

PACS: 23.40.Bw, 23.40.-s, 14.60.Pq, 21.60.Cs

Key words: incoherent muon–electron conversion rate, spurious center-of-mass excitation, continuum-RPA method

1 Introduction

Theories that go beyond the Standard Model (SM) of particle physics allow for the violation of various symmetries respected by the SM, among which the conservation of lepton flavour. Evidence for lepton flavour violation (LVF) has been provided by the neutrino oscillation experiments. In the charged-lepton sector, processes that would provide additional evidence for LVF and help distinguish among the various proposed mechanisms, include the exotic neutrinoless conversion of a muon to an electron — where the neutrino and antineutrino involved in the conversion are assumed to be Majorana particles and can annihilate each other.

In this context, the exotic conversion of a bound muon to an electron

$$\mu^- + (A, Z) \rightarrow e^- + (A, Z)^* \quad (1)$$

^{*)} Presented by P. Papakonstantinou at the Workshop on calculation of double-beta-decay matrix elements (MEDEX'05), Corfu, Greece, September 26–29, 2005.

has been studied both experimentally and theoretically [1–10]. The experimentally measured quantity is the ratio of the coherent rate, where the nucleus remains in its ground state, over the total capture rate. Although the coherent rate dominates the capture rate (accounting for about 90% of it), in order to calculate this ratio and make meaningful comparisons with experiment, both the coherent and the incoherent rate need to be evaluated theoretically.

Various methods have been employed for the calculation of the incoherent $\mu^- - e^-$ conversion rate [4, 7–14]. State-by-state calculations performed within the shell model and the quasiparticle RPA (QRPA) indicate that

1. the main contribution to the incoherent rate comes from low-lying states,
2. the contribution of the 1^- channel is very large (about 50%, for all mechanisms leading to $\mu^- - e^-$ conversion). Therefore, it is essential to properly remove possible spurious center-of-mass (CM) contaminations.

In a recent paper [15] we used a Continuum-RPA (CRPA) method with Skyrme interactions to address the question as to how insignificant the contribution of excited states lying high in the continuum really is. We considered natural-parity excitations of the ^{208}Pb nucleus and found that high-lying strength is not negligible. In this work we continue this investigation by looking at a lighter nucleus as well, namely ^{40}Ca . For both nuclei we also examine in detail the admixture of spurious components in the rate coming from 1^- excitations. To this end we have used both the self-consistent CRPA and a non-consistent version (ncRPA) and have employed two ways to remove the spurious strength: by using effective dipole operators, as done in Ref. [15] for ^{208}Pb , and by simply throwing away the spurious state appearing close to zero energy. In both cases, the correction achieved is quite large.

Useful definitions and basic information on the methods are provided in Sect. 2. In Sect. 3 we apply our CRPA method, which takes the full continuum into account, to the nuclear targets ^{208}Pb and ^{40}Ca . The spurious strength is discussed in detail in Subsect. 3.2. We conclude in Sect. 4.

2 Definitions and method of calculation

The inclusive (μ^-, e^-) rate is evaluated by summing the partial contribution of all final states $|f\rangle$. For spherical or nearly spherical nuclei, the vector contribution is given by [4]

$$S_a = \sum_f \left(\frac{q_f}{m_\mu} \right)^2 |\langle f | O_a(\mathbf{q}_f) | 0 \rangle|^2, \quad (2)$$

where $O_a(\mathbf{q}_f)$ represents the vector-type transition operator resulting in the context of a given mechanism mediated by a photon ($a = \gamma$), a W -boson ($a = W$) or a Z -particle exchange ($a = Z$). Here \mathbf{q}_f , with magnitude $q_f = m_\mu - \epsilon_b - E_f$, is the momentum transferred to the nucleus. E_f is the energy of the final state $|f\rangle$ with

respect to the ground state $|0\rangle$, ϵ_b is the binding energy of the muon and m_μ its mass. The transition operators have the form

$$O_a(\mathbf{q}) = \tilde{g}_V f_V \sum_{j=1}^A 6c_a(\tau_j) e^{-i\mathbf{q}\cdot\mathbf{r}_j}, \quad c_a(\tau_j) \equiv \frac{1}{2} + \frac{1}{6}\beta_a\tau_j, \quad (3)$$

where τ_j is the 3rd component of the j th particle's isospin. The parameter $f_V = 1.0$ represents the vector static nucleon form factor and the normalization coefficient \tilde{g}_V takes the value $1/6$ for the photonic case and $1/2$ for the non-photonic W -boson and SUSY Z exchange [5]. The value of β_a depends on the model assumed. We have adopted the values from Ref. [8]. Thus, protons (neutrons) contribute to a given process with a "charge" whose value is determined by $c_a(1/2) = 1/2 + \beta_a/6$ ($c_a(-1/2) = 1/2 - \beta_a/6$). In the photon and Z case, the isoscalar and isovector components of the transition operator are (almost) equally important, whereas O_W is predominantly isoscalar.

By assuming that the initial and final states are of definite spin and parity, a multipole decomposition of the operators of Eq. (3) into operators T_{aLM} of orbital angular momentum rank L can be carried out. For spherical nuclei we can assume, without loss of generality, $\hat{q} = \hat{z}$. Then, only terms with $M = 0$ survive, for which we obtain ($T_{aL}(q) \equiv T_{aL0}(q)$)

$$T_{aL}(q) = \tilde{g}_V f_V \sqrt{4\pi(2L+1)} \sum_{j=1}^A 6c_a(\tau_j) j_L(qr_j) Y_{L0}(\hat{r}_j). \quad (4)$$

A phase factor $(-i)^L$ has been omitted. The contribution of each multipolarity to the transition rate S_{aL} reads

$$S_{aL} = \sum_f \left(\frac{q_f}{m_\mu} \right)^2 |\langle f | T_{aL}(q_f) | 0 \rangle|^2. \quad (5)$$

We now rewrite the rate S_{aL} as the integral of a suitable distribution over excitation energy:

$$S_{aL} \equiv \int dE R_{aL}(E) \quad (6)$$

with

$$R_{aL}(E) = \left(\frac{E^2}{m_\mu^2} - 2k \frac{E}{m_\mu} + k^2 \right) R'_{aL}(E). \quad (7)$$

In the above expression we have set $k \equiv 1 - \epsilon_b/m_\mu$, while

$$R'_{aL}(E) = \sum_f |\langle f | T_{aL}(m_\mu - \epsilon_b - E_f) | 0 \rangle|^2 \delta(E - E_f) \quad (8)$$

stands for the "strength distribution" corresponding to the operator $T_{aL}(q)$, with $q = m_\mu - \epsilon_b - E$.

The final states $|f\rangle$, excited by the single-particle operator T_{aL} , are of particle-hole (ph) type. Then, the distribution $R'_{aL}(E)$, and from it $R_{aL}(E)$, can be cal-

culated following the standard RPA method. Subsequently, Eq. (6) can be used to evaluate the total rate S_{aL} .

We consider ph excitations, built on top of the mean-field ground state of a closed-shell nucleus and subjected to the ph residual interaction. In particular, the quantities introduced above are calculated using a self-consistent Skyrme–Hartree–Fock (SHF) plus Continuum-RPA (CRPA) model. The HF equations describing the ground state are derived variationally from the Skyrme energy functional. RPA excitations are considered on top of the HF ground state. The CRPA is formulated in coordinate space, so that the full particle continuum is taken into account. The same Skyrme interaction is used to calculate the ground state properties and the residual ph interaction. The model is described in detail in Ref. [15] and references therein. In this work we have employed the SkM*[17] parametrization of the Skyrme force. It describes satisfactorily giant resonances of stable nuclei, and therefore it is suitable for the present study. In order to test the sensitivity of our results on the interaction used, we have also used MSk7 [18], which has a large effective mass, thereby shifting most excited states to lower energies compared to the more reliable SkM*.

For the purposes of Subject. 3.2 we have employed also the non-consistent CRPA version (ncRPA) of Ref. [19] and the corresponding numerical code [20]. The ground state is described by a Woods–Saxon potential of radius $(A-1)^{1/3}r_0$ ($r_0 = 1.25$ fm) and diffuseness $a_0 = 0.65$ fm, including central (strength $V_0 = -53$ MeV), spin-orbit ($V_{so} = 15.5$ MeV fm²), symmetry ($V_T = 20$ MeV) and Coulomb terms. The residual ph interaction is a simplified Skyrme interaction without spin and velocity dependence ($t_0 = -1100$ MeV fm³, $x_0 = 0.5$, $t_3 = 15000$ MeV fm⁶). Its strength is scaled by a factor V_{scal} so as to bring the spurious state close to zero energy.

Results are presented and discussed in the next section.

3 Results

Next, we present results for the nuclei ²⁰⁸Pb and ⁴⁰Ca. The muon binding energy in ²⁰⁸Pb is $\epsilon_b = 10.475$ MeV. The particle threshold energy E_{thr} is 8.09 MeV in the case of the SkM* force. The respective values for ⁴⁰Ca are $\epsilon_b = 1.0533$ MeV, $E_{thr} = 8.86$ MeV. We have obtained results for $L = 0, 1, \dots, 6$ and for natural parity, $(-1)^L$. The most important contributions to the incoherent transition rate are expected from $L < 4$ [10].

3.1 Incoherent transition rate in the continuum

In Fig. 1, above two panels, the distribution $R_{aL}(E)$ is plotted as a function of E , for the 0^+ and 4^+ transitions of ²⁰⁸Pb. For the 1^- distribution of ²⁰⁸Pb the reader is referred to Fig. 4 (upper-left panel, full lines) in the next subsection. In the monopole case, $L = 0$, the Isoscalar (IS) Giant Monopole Resonance (GMR) is the main peak. For γ and Z, there is considerable contribution coming from higher energies (20–35 MeV), i.e. the isovector (IV) GMR region. For $L = 1$, the IV Giant Dipole Resonance (GDR) corresponds to the strength clustered around

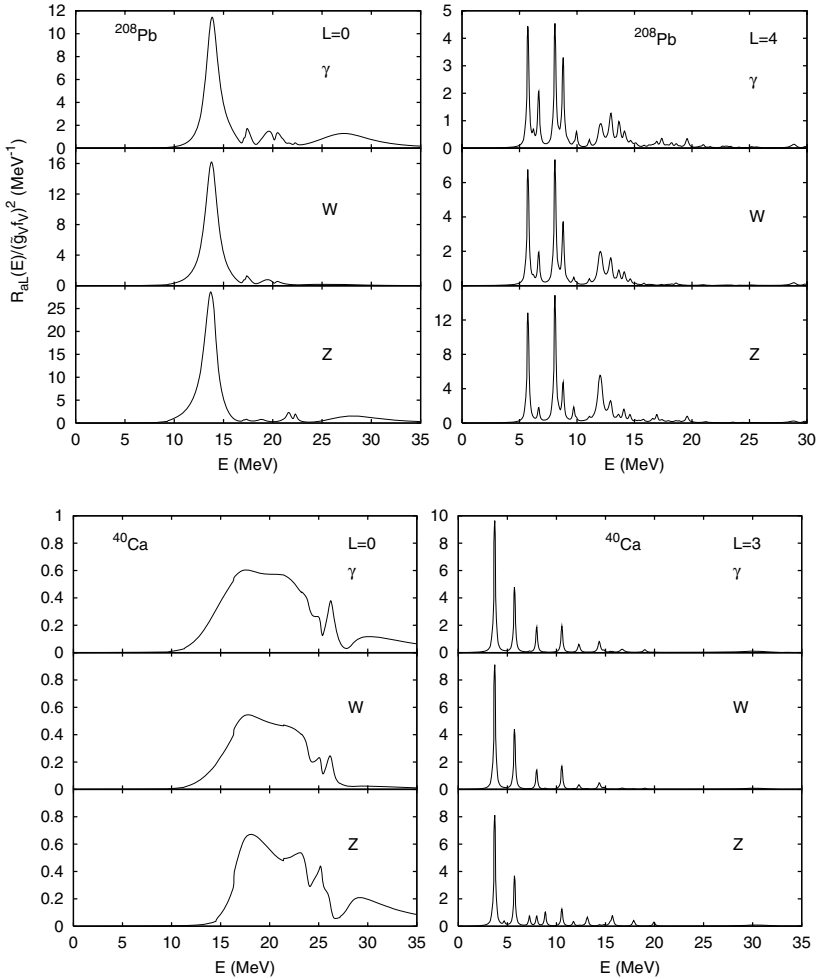


Fig. 1. The distribution $R_{\alpha L}(E)$ in ^{208}Pb for $L = 0, 4$ and in ^{40}Ca for $L = 0, 3$. Skyrme parameterization SkM* has been used.

$E \approx 12$ MeV. For W and Z , important contribution seems to come from higher energies (above 20 MeV), in particular, the IS GDR. For W exchange, the region below 10 MeV contributes significantly. In this region we find the oscillation of the neutron skin against the nuclear core (pygmy dipole resonance) [16]. In the quadrupole case, $L = 2$ (not shown), both the IS Giant Quadrupole Resonance (GQR), close to 11 MeV, and the collective low-lying state are strong. There is some contribution from energies higher than 15 MeV, i.e. from the IV GQR region, especially in the cases γ and Z . For $L = 3$ (not shown) the strength is mostly concentrated in the collective octupole state at low energy. For $L > 3$, e.g. for $L = 4$ in Fig. 1, the calculated strength is quite fragmented and most of it lies below 20 MeV.

In Fig. 1, bottom two panels, the distribution $R_{aL}(E)$ is plotted as a function of E , for the 0^+ and 3^- transitions of ^{40}Ca . For the 1^- distribution of ^{40}Ca the reader is referred to Fig. 4 (upper-right panel, full lines) in the next subsection. The monopole strength distribution is dominated by the broad IS GMR. Above 27 MeV the IV GMR is excited through the γ and Z mechanisms. The IV GDR dominates the dipole spectrum. In the 2^+ distribution we find the strong IS GQR at about 17 MeV and seemingly little strength at higher energies. The 3^- , 4^+ (not shown) distributions are quite fragmented. A strong peak appears at about 5 MeV in the 5^- distribution (not shown) along with fragmented strength at higher energies. In the 6^+ distribution (not shown) we find a strong peak at around 15 MeV and a broad structure in the continuum between 20 and 30 MeV.

In Fig. 2 we plot the fraction of the total strength S_{aL} coming from states below the particle threshold ($S_{aL,\text{thr}}$) and the fraction coming from states below 20 MeV ($S_{aL,20\text{MeV}}$), vs. the multipolarity L , for ^{208}Pb and using the Skyrme parametrizations SkM* and MSK7. We see that for low multipoles $L = 0, 1, 2$ only a small portion of the strength originates from energies below particle threshold. The trend followed is similar for all mechanisms and independent of the interaction used. For

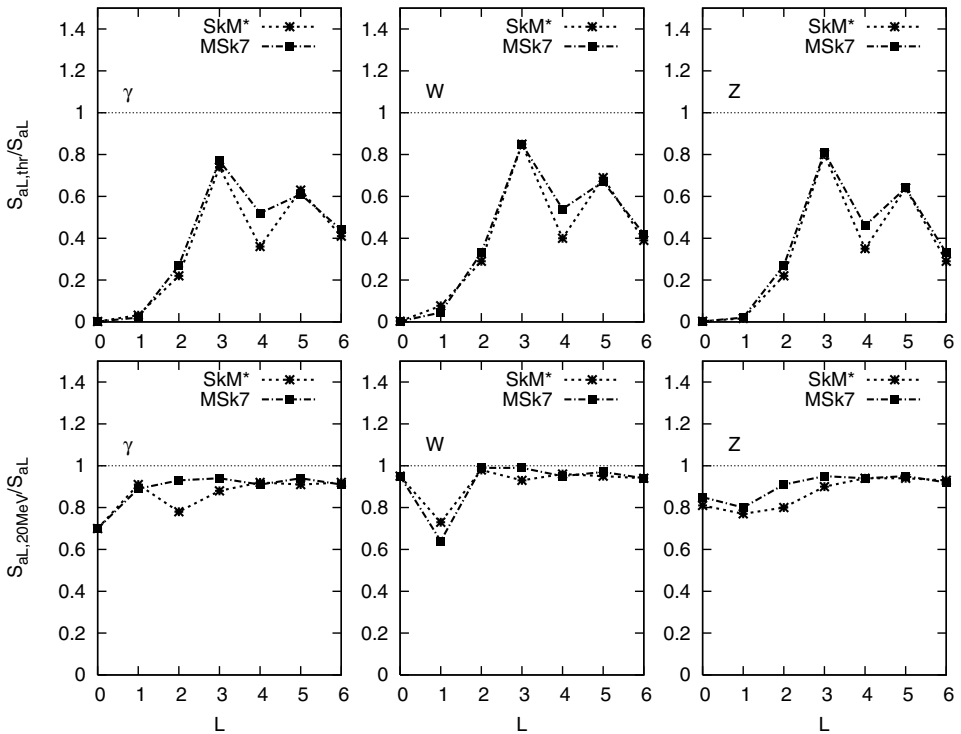


Fig. 2. Fraction of the total strength S_{aL} , for the nucleus ^{208}Pb , coming from states below the particle threshold (top) and below 20 MeV (bottom) vs the multipolarity L . Skyrme parameterizations SkM* and MSK7 have been used. Lines are drawn to guide the eye.

even multipoles $L = 2, 4$ a big portion of the contribution is pushed to higher energies as compared to the neighboring odd ones. For some multipoles ($L = 0$ for photonic mechanism, $L = 1$ for W -boson exchange), a significant portion of the strength comes from above 20 MeV.

In Fig. 3 we show the fractions $S_{aL,thr}/S_{aL}$ and $S_{aL,20\text{MeV}}/S_{aL}$ for both nuclei ^{208}Pb and ^{40}Ca , evaluated using the SkM* force. We also show, for ^{40}Ca , the fraction $S_{aL,35\text{MeV}}/S_{aL}$ coming from states below 35 MeV. The quantities $S_{aL,thr}/S_{aL}$ for ^{40}Ca show that for $L = 0, 1$ and, in addition, for $L = 2, 4, 6$ almost all of the strength comes from above threshold. One should bear in mind that ^{40}Ca is an ℓ -closed nucleus, without low-lying $\Delta N = 0$ ph states. ^{208}Pb , on the other hand, is ℓj -closed and low-lying $L = 2, 4, 6$ transitions between spin-orbit partners are present. For odd multipoles in ^{40}Ca an important amount of strength comes from continuum excitations as well. A larger fraction of strength is found above 20 MeV for ^{40}Ca than for ^{208}Pb . In this sense, high-lying excitations are found more important for ^{40}Ca than for ^{208}Pb . Of course, the value of $E_{\text{max}} = 20\text{ MeV}$

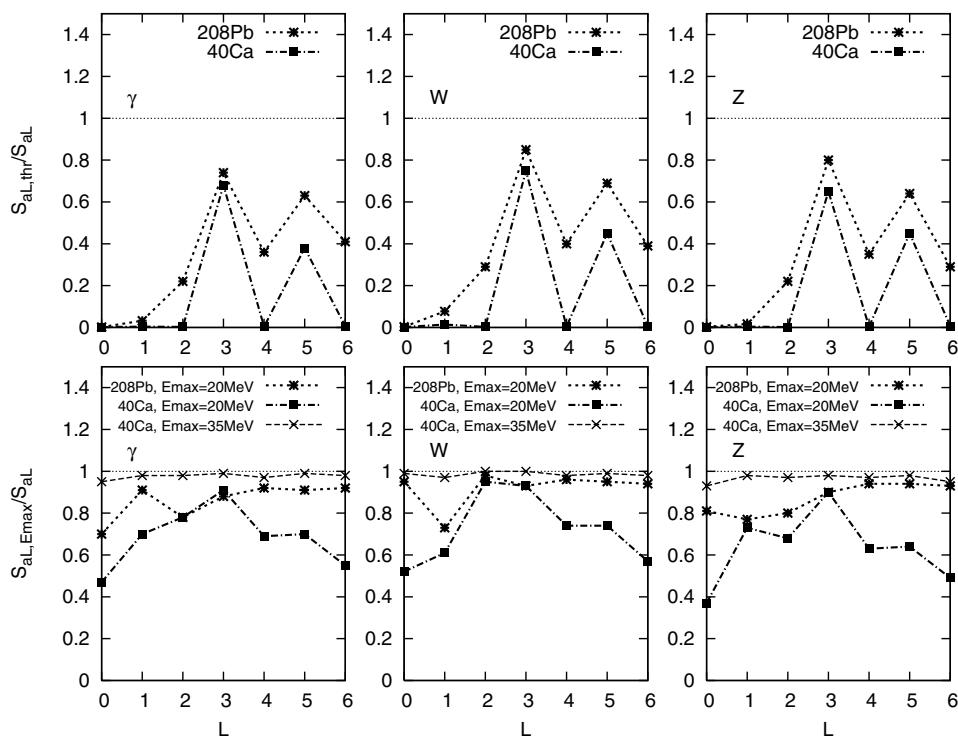


Fig. 3. Fraction of the total strength S_{aL} , for the nuclei ^{208}Pb and ^{40}Ca , coming from states below the particle threshold (top) and below 20 MeV (bottom) vs the multipolarity L . For ^{40}Ca the fraction of strength coming from below 35 MeV is also shown (bottom).

Skyrme parameterization SkM* has been used. Lines are drawn to guide the eye.

was chosen arbitrarily. The oscillator level spacing ($\hbar\omega \approx 41A^{-1/3}$) of a light nucleus is larger than for a heavier nucleus and the energies of the corresponding excitations are higher. If we choose to compare, e.g., the $S_{aL,20\text{MeV}}/S_{aL}$ of ^{208}Pb with the $S_{aL,35\text{MeV}}/S_{aL}$ of ^{40}Ca (the maximum energy being ≈ 3 shells in both cases), we find that, in the latter case, values closer to unity are reached.

We have calculated also the fraction of the total strength S_{aL} , coming from states below 50 MeV, for L up to 6 and for both nuclei. In all cases, the fraction is practically equal to unity. This means that the discretized versions of RPA and QRPA are safe to use if the energy cutoff is large enough to sufficiently account for transitions below this value.

3.2 Removal of spurious strength

It is well known [12, 13] that the 1^- excitations contain admixtures of the spurious excitation of the center of mass (CM) of the nucleus, corresponding to a situation in which the nucleus moves as a whole around the localized fictitious potential well. Normally, spurious components are separated out by the RPA methods. However, the use of a truncated model space and non-self-consistent single particle energies in ordinary RPA and the other versions of QRPA destroys the translational invariance and inserts spurious excitations into the spectrum. Thus, the spurious CM state is not completely separated from the real (intrinsic) nuclear excitations, and in addition its energy eigenvalue is not zero. In Continuum-RPA models with Skyrme interactions it has been possible to achieve a high degree of self-consistency, i.e. the same interaction is used for the HF calculation of ground state properties and for the residual interaction. In addition, no truncation is involved. However, due to the formulation of the model in coordinate space, it is common practice to exclude the Coulomb and spin-orbit contribution (at least) to the residual interaction. Therefore, self-consistency is violated and, even in cases where the spurious state appears very close to zero energy, some spurious strength may remain at higher energies.

For electric dipole excitations, the problem is usually treated by using effective charges [22]. Similarly, in the case of IS dipole excitations, effective operators are used [23, 24], which minimize the spurious admixture in the strength distribution. (The effect on the IS dipole excitations of ^{208}Pb was examined in detail in Ref. [25].) In Ref. [15] we presented a similar prescription for the operators involved in $\mu^- - e^-$ conversion. In particular, the operators T_{a1} which induce the 1^- excitations,

$$T_{a1}(q) = \sum_{j=1}^A c(\tau_j) f(r_j) Y_{10}(\hat{r}_j); f(r) = 6\tilde{g}_V f_V \sqrt{12\pi} j_1(qr), \quad (9)$$

are replaced by respective effective operators

$$T_{a1}^{\text{corr}}(q) = \sum_{j=1}^A [c(\tau_j) f(r_j) - \eta_a r_j] Y_{10}(\hat{r}_j). \quad (10)$$

In principle, the operators T_{a1} and T_{a1}^{corr} induce the same intrinsic excitations, because they only differ by a term which translates the center of mass. The parameter η_a in Eq. (10) is determined so as to eliminate the spurious CM excitation within the collective model. One finds [15]

$$\eta_a = \tilde{g}_V f_V 4\sqrt{3\pi}q \left[\frac{c_a \left(\frac{1}{2}\right) Z}{A} F_p(q) + \frac{c_a \left(-\frac{1}{2}\right) N}{A} F_n(q) \right]. \quad (11)$$

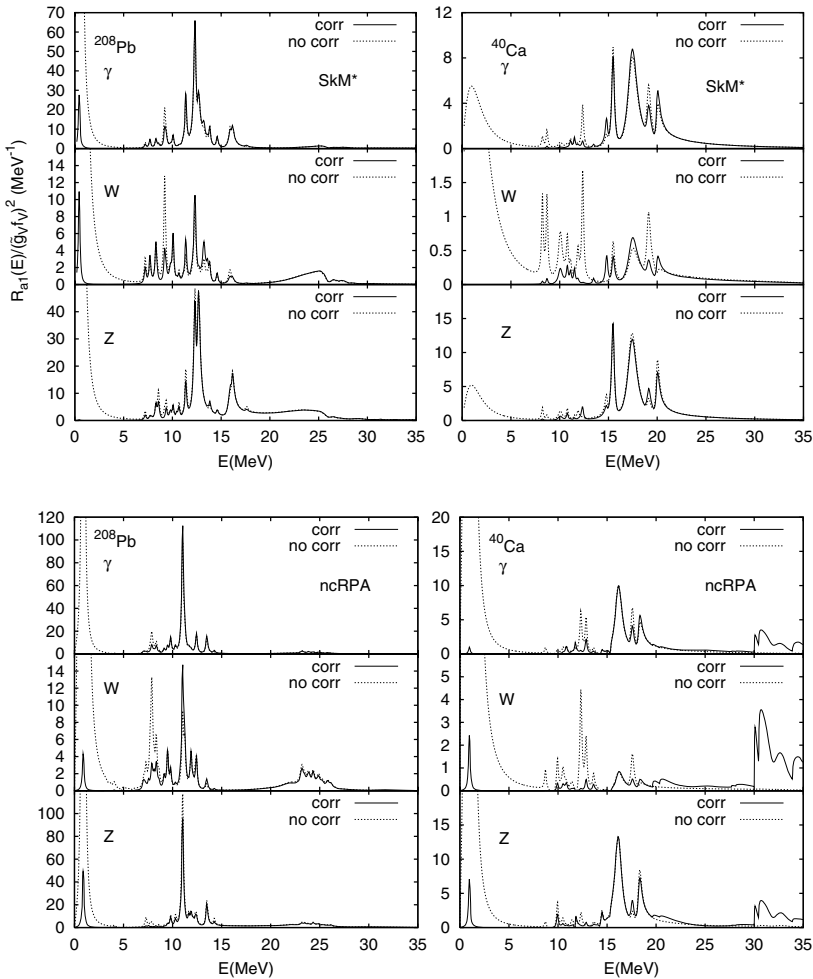


Fig. 4. The dipole distributions $R_{a1}(E)$, for γ -photon and W -boson exchange diagrams of the $\mu^- \rightarrow e^-$ conversion in ^{208}Pb and ^{40}Ca . The results have been calculated for the dipole operator T_{a1} (dotted line) and for the corresponding corrected operator given by Eqs. (10), (11). Upper panels: The self-consistent CRPA with Skyrme parametrization SkM* was used. Bottom panels: the non-self-consistent RPA was used.

The point-proton and neutron form factors, $F_p(q)$ and $F_n(q)$, respectively, are calculated numerically using the ground-state densities.

In Fig. 4, upper panels, we plot the dipole distributions $R_{a1}(E)$, for photon, W - and Z -boson exchange diagrams, calculated by using the corrected and uncorrected operator. The SkM* interaction was used. Results are shown for both ^{208}Pb and ^{40}Ca . Most of the spurious strength below ≈ 6 MeV has been removed. The strength distributions above 20 MeV are practically unaffected. The strength in the region of the IVD resonance appears redistributed. The effect of the correction appears strongest in the case of the W -boson exchange mechanism and for ^{40}Ca . The pygmy dipole state of ^{208}Pb below 10 MeV is strongly affected by the correction in the photonic and W cases.

In most of the cases, the effect of the correction above the tail of the spurious state appears small. Therefore, it would have been a fairly good approximation to simply throw away the spurious state and calculate the transition rate coming from states above, approximately, 6 MeV. Such an approximation was used in Ref. [10]. One should keep in mind, however, that our CRPA model is self-consistent to a high degree. Thus, the excitation spectrum above the spurious state is almost free of spurious components, already before the operator correction, and therefore almost insensitive (up to 10%, as we will see) to the change of operators. This is not necessarily the case in less consistent models such as the one in Ref. [10] and the ncRPA model described in Sect. 2.

Next we employ the ncRPA method and calculate again the $R_{a1}(E)$ distributions using the operators T_{a1} and T_{a1}^{corr} . In the case of ^{208}Pb (^{40}Ca) the residual interaction was scaled by a factor $V_{\text{scal}} = 0.94$ (1.004) in order to bring the spurious state close to zero energy. The results are shown in Fig. 4, bottom panels. Again, in all cases, most of the strength of the spurious state is eliminated. In general, the effect appears small for ^{208}Pb , above the tail of the spurious state. The pygmy dipole state is strongly affected and the strength of the IS GDR is slightly reduced (see W -boson mechanism). For ^{40}Ca the effect appears small in the region of the IV GDR, but not below and above. In particular, the use of corrected operators results in significant additional strength above 20 MeV. In total, the transition strength above the spurious state (above 6 MeV) increases. The sensitivity of the calculation on the operators used implies a bad degree of consistency which renders the calculation unreliable.

In Table 1 we list, for both nuclei, i) the portion $s_{\text{tot}}^{\text{sp}}$ of transition strength removed from the total contaminated 1^- transition strength S_{a1} when corrected operators T_{a1}^{corr} are employed, ii) the portion of strength S_{sp} carried by the spurious state when the uncorrected T_{a1} operators are used (calculated as the portion of strength lying below 6 MeV), and iii) the portion $s_{>6}^{\text{sp}}$ MeV of the strength removed from above 6 MeV excitation energy when corrected operators are used (with respect to the uncorrected strength above 6 MeV). Results have been obtained with both models, i.e. our self-consistent CRPA model with interaction SkM* and the non self-consistent CRPA model labelled ncRPA.

Let us first examine the behavior of the self-consistent CRPA model. As the values of $s_{\text{tot}}^{\text{sp}}$ show, about 90% of the total transition rate was spurious in all cases.

Table 1. Percentage of the total 1^- transition strength S_{a1} ($s_{\text{tot}}^{\text{sp}}$) and of the strength above 6 MeV ($s_{>6\text{MeV}}^{\text{sp}}$) consumed by spurious transitions, and percentage of strength below 6 MeV (\approx strength of the spurious state, S_{sp}) for the three channels γ , W , Z . Results are shown for the nuclei ^{208}Pb and ^{40}Ca obtained by using two models: the self-consistent Continuum RPA with Skyrme force SkM* and the non-consistent RPA (ncRPA). Last row: When corrected operators are used in this case, the strength above 6 MeV increases significantly. Square brackets: the energy of the spurious state is found imaginary, therefore its strength is not properly evaluated.

		γ	W	Z
$s_{\text{tot}}^{\text{sp}}$ (%)	^{208}Pb -SkM*	86.9	96.3	90.5
	^{208}Pb -ncRPA	89.8	96.5	88.5
	^{40}Ca -SkM*	[33.8]	[82.0]	[28.6]
	^{40}Ca -ncRPA	90.8	93.7	88.0
S_{sp} (%)	^{208}Pb -SkM*	88.0	96.6	89.9
	^{208}Pb -ncRPA	90.0	96.5	90.3
	^{40}Ca -SkM*	[29.0]	[67.7]	[21.6]
	^{40}Ca -ncRPA	95.2	98.7	93.6
$s_{>6\text{MeV}}^{\text{sp}}$ (%)	^{208}Pb -SkM*	-1.3	7.8	6.1
	^{208}Pb -ncRPA	-1.6	12.5	16.2
	^{40}Ca -SkM*	6.7	45.0	9.1
	^{40}Ca -ncRPA	incr.	incr.	incr.

We expect this result to be independent of the nucleus and the interaction used, because the spurious state at low energy always dominates the isoscalar dipole strength distribution (which contributes in all the three mechanisms) and because the corrected operators are, by construction, most effective for this state (thus removing practically all its strength). We were not able to demonstrate this in the particular case of ^{40}Ca , because the energy of the spurious state in this case was found imaginary. In other words, we were not able to evaluate and take into account properly the strength of the spurious state, before or after the correction. Therefore, the respective numbers in Table 1 are placed in brackets.

Suppose now that, in order to evaluate the rate coming from intrinsic 1^- excitations, we would apply the procedure of using the T_{a1} operators and then simply excluding the strength of the spurious state from calculating the total rate. As the values of S_{sp} show, for ^{208}Pb , we would have removed roughly as large a portion as $s_{\text{tot}}^{\text{sp}}$. Again, for ^{40}Ca it is not possible to conclude.

From Table 1 we notice that for $s_{>6\text{MeV}}^{\text{sp}}$ and for $a = \gamma$ the result is small in absolute value, but negative, for ^{208}Pb . It represents the numerical accuracy of our calculation and, being small, it indicates that the degree of self-consistency reached by our HF+CRPA model is sufficient to achieve a satisfactory separation of the spurious transition in this case. For the W and Z cases, however, spurious admixtures of more than 6% are found above 6 MeV. These numbers (which are not free of numerical inaccuracies, as explained in Ref. [15]) vary when different

Skyrme interactions are used, with their values remaining below 10%. In the case of ^{40}Ca , the values of $s_{>6\text{MeV}}^{\text{SP}}$ for the γ and Z mechanisms are lower than 10% as well. Its value for W -exchange is much larger. Most of it, however, comes from below 15 MeV (below the GDR region).

When the ncRPA model is used, similar results are obtained for $s_{\text{tot}}^{\text{SP}}$ and S_{sp} as with the self-consistent model. The ^{208}Pb excitation spectrum above the tail of the spurious state is more contaminated than within the self-consistent CRPA, as the $s_{>6\text{MeV}}^{\text{SP}}$ values show. As for the ^{40}Ca nucleus, when corrected operators were used, the strength above 6 MeV was significantly increased. Thus, the corresponding values of $s_{>6\text{MeV}}^{\text{SP}}$ are large and negative, indicating a bad performance of the model.

From our results, obtained for two nuclei within two different continuum-RPA models, one may conclude that more than 85% of the total 1^- rate, when no correction is considered, is spurious. Whether effective operators are used to remove the total spurious strength, or whether one excludes the spurious state from the calculation of the total 1^- , the above conclusion remains the same. This does not mean that there are no spurious contaminations above the zero-energy spurious mode. When making use of corrected operators, the strength of the excited states across the spectrum is redistributed. The overall effect, however, is to reduce the total S_{a1} rate by the amount that was initially carried by the spurious state.

Within the QRPA calculations of Ref. [10], for six nuclei (including ^{208}Pb), a more moderate correction (less than 60%) on S_{a1} was achieved by considering the lowest 1^- state as purely spurious and simply excluding it. One should keep in mind the differences between the models used there (QRPA calculations with a renormalized G -matrix interaction) and the ones used here. First of all, priority was given in Ref. [10] to the best possible reproduction of experimental spectra, rather than controlling the self-consistency. In addition, a truncated model space was used, contrary to the methods used in the present work. The various approximations entering may have influenced the spuriosity results in an unpredictable way. Both consistency and completeness of the space are important in order to move as much spurious strength as possible close to zero energy. Of course, the lowest 1^- state appeared very close to zero energy. It was found that it was spurious by (60–80)% (except for ^{126}Yb , for which it was about 90% spurious). Thus, the approximation of considering it as purely spurious is not a very good one. The numbers mentioned above refer to the overlap of the lowest 1^- state with the “purely spurious” RPA state. Approximations were inevitable when constructing the purely spurious state, in order to normalize it.

4 Conclusions

We have investigated the incoherent rate of the exotic $\mu^- - e^-$ conversion in the nuclei ^{208}Pb and ^{40}Ca . We employed the Continuum-RPA method which is appropriate for explicit construction of the excited states lying in the continuum spectrum of the nuclear target. We used a self-consistent CRPA and Skyrme interactions to investigate the transition strength coming from natural-parity ph excitations. We found that a significant portion of the incoherent $\mu^- - e^-$ rate comes from high-lying

nuclear excitations. The admixture of spurious components in the rate coming from 1^- excitations was investigated in detail by using the self-consistent CRPA with Skyrme interactions as well as a less consistent version of CRPA and by employing two ways to remove the spurious strength: the use of effective operators or simply the exclusion of the spurious state appearing close to zero energy. In all cases, we found that the greatest portion of the 1^- transition strength is due to the spurious CM excitation, a result in agreement with that of an exact method constructed recently [14] for removing spurious contaminations.

This work has been supported by the Deutsche Forschungsgemeinschaft under contract SFB 634 and by the Hellenic General Secretariat for Research and Technology (www.gsrt.gr) under Program PENED-03 (Space Sciences and Technologies). T.S.K. acknowledges partial support from the IKYDA-02 Greece–Germany project. P.P. acknowledges support from the ILIAS-N6 EU project for participation to the MEDEX-05 meeting.

References

- [1] A. van der Schaaf: Prog. Part. Nucl. Phys. **31** (1993) 1.
- [2] W. Molzon: in *Symmetries in Intermediate and High Energy Physics*, (Eds. A. Faessler, T.S. Kosmas, and G.K. Leontaris), Springer Tracts in Mod. Phys., Vol. **163**, Springer-Verlag, Berlin–New York, 2000, p. 105.
- [3] Y. Kuno and S. Okada: Rev. Mod. Phys. **73** (2001) 151.
- [4] T.S. Kosmas, Nucl. Phys. A **683** (2001) 443; Prog. Part. Nucl. Phys. **48** (2002) 307; NIM Phys. Res. A **503** (2003) 247.
- [5] T.S. Kosmas, A. Faessler, and J.D. Vergados: J. Phys. G **23** (1997) 693.
- [6] R. Kitano, M. Koike, and Y. Okada: Phys. Rev. D **66** (2002) 096002.
- [7] T.S. Kosmas and J.D. Vergados: Phys. Rep. **264** (1996) 251.
- [8] T. Siiskonen, J. Suhonen, and T.S. Kosmas: Phys. Rev. C **60** (1999) 062501(R); **62** (2000) 035502.
- [9] T.S. Kosmas, A. Faessler, F. Šimkovic, and J.D. Vergados: Phys. Rev. C **56** (1997) 526.
- [10] J. Schwieger, A. Faessler, and T.S. Kosmas: Phys. Rev. C **56** (1997) 2830.
- [11] H.C. Chiang, E. Oset, T.S. Kosmas, J.D. Vergados, and A. Faessler: Nucl. Phys. A **559** (1993) 526.
- [12] J. Meyer-ter-Vehn: Z. Phys. A **289** (1979) 319.
- [13] N.I. Pyatov and M.I. Baznat: Sov. J. Nucl. Phys. **30** (1979) 634.
- [14] D.R. Bes and O. Civitarese: Phys. Rev. C **63** (2001) 044323.
- [15] P. Papakonstantinou, T.S. Kosmas, J. Wambach, and A. Faessler: Phys. Rev. C **73** (2006) 035502.
- [16] Y. Suzuki, K. Ikeda, and H. Sato: Prog. Theor. Phys. **83** (1990) 180.
- [17] J. Bartel, P. Quentin, M. Brack, C. Guet, and H.-B. Hakansson: Nucl. Phys. A **386** (1982) 79.

- [18] S. Goriely, F. Tondeur, and J.M. Pearson: *At. Data Nucl. Data Tables* **77** (2001) 311.
- [19] S. Shlomo and G.F. Bertsch: *Nucl. Phys. A* **243** (1975) 507.
- [20] G. Bertsch: in *Computational Nuclear Physics I – Nuclear Structure*, (Eds. K. Langanke, J.E. Maruhn, and S.E. Koonin), Springer, New York, 1991, p. 75.
- [21] S. Shlomo, V.M. Kolomietz, and B.K. Agrawal: *Phys. Rev. C* **68** (2003) 064301.
- [22] A. Bohr and B.R. Mottelson: *Nuclear Structure – Vol. I*, Benjamin, New York–London, 1969.
- [23] N. Van Giai and H. Sagawa: *Nucl. Phys. A* **371** (1981) 1.
- [24] B.K. Agrawal, S. Shlomo, and A.I. Sanzhur: *Phys. Rev. C* **67** (2003) 034314.
- [25] I. Hamamoto and H. Sagawa: *Phys. Rev. C* **66** (2002) 044315.